A maximum likelihood proton path formalism for application in proton computed tomography

R. W. Schulte[a)]
Department of Radiation Medicine, Loma Linda University Medical Center, Loma Linda, California 92354

S. N. Penfold
Centre for Medical Radiation Physics, University of Wollongong, Wollongong, NSW 2522, Australia

J. T. Tafas and K. E. Schubert
Department of Computer Science and Engineering, California State University, San Bernardino, California 92407

(Received 5 May 2008; revised 20 August 2008; accepted for publication 25 August 2008; published 13 October 2008)

The limited spatial resolution in proton computed tomography (pCT) in comparison to x-ray CT is related to multiple Coulomb scattering (MCS) within the imaged object. The current generation pCT design utilizes silicon detectors that measure the position and direction of individual protons prior to and post-traversing the patient to maximize the knowledge of the path of the proton within the imaged object. For efficient reconstruction with the proposed pCT system, one needs to develop compact and flexible mathematical formalisms that model the effects of MCS as the proton traverses the imaged object. In this article, a compact, matrix-based most likely path (MLP) formalism is presented employing Bayesian statistics and a Gaussian approximation of MCS. Using GEANT4 simulations in a homogeneous 20 cm water cube, the MLP expression was found to be able to predict the Monte Carlo tracks of 200 MeV protons to within 0.6 mm on average when employing 3σ cuts on the relative exit angle and exit energy. These cuts were found to eliminate the majority of events not conforming to the Gaussian model of MCS used in the MLP derivation. © *2008 American Association of Physicists in Medicine*. [DOI: 10.1118/1.2986139]

Key words: Proton computed tomography, most likely path formalism, spatial resolution

I. INTRODUCTION

Proton radiography and proton computed tomography (pCT) were first proposed as a possibility by Cormack[1] in 1963 and later explored experimentally.[2–7] Through these studies a number of advantages of pCT over conventional x-ray CT (xCT) were identified. However, one limiting factor and a major reason for the abandonment of the early experimental projects was the obvious lack of spatial resolution achievable with pCT in comparison to xCT. This substandard spatial resolution is related to multiple Coulomb scattering (MCS) within the imaged object. In MCS the protons interact with the Coulomb fields of the nuclei in the absorbing material, resulting in many small-angle deflections in the proton trajectory.

With the expansion of proton radiation therapy since the 1990's, renewed interest has been placed in the development of a clinical pCT system.[7–9] The current generation pCT design utilizes silicon detectors that measure the position and direction of individual protons prior to and post-traversing the patient to maximize the knowledge of the path of the proton within the imaged object.[8] With such knowledge, electron density maps can be reconstructed with submillimeter spatial resolution using iterative reconstruction algorithms.[9] For efficient pCT reconstruction one needs to develop compact and flexible mathematical formalisms that model the effects of MCS as the proton traverses the imaged object.

There have been two primary studies in which mathematical formulas were published that attempted to model the effects of MCS on proton trajectory while traversing a uniform material. The first, by Schneider and Pedroni,[10] was formulated for analysis of spatial resolution in proton radiography. This formalism, based on the generalized Fermi-Eyges theory of MCS,[11] sought to calculate the most probable trajectory of protons and its standard deviation at any intermediate depth in an absorber having measured a certain entry and exit location, and was expanded upon to include scenarios wherein the exit direction of the proton was also known. Williams,[12] assuming knowledge of entry and exit position and exit direction, later went on to use χ^2 statistics to derive a most likely path (MLP) formalism including error envelopes for pCT application. The advantage in terms of spatial resolution achievable in pCT reconstructed images when employing Williams's MLP formalism in combination with an algebraic reconstruction algorithm was demonstrated by Li *et al.*[9] A drawback of Williams's formalism, however, is that it cannot directly be applied to scenarios in which only incomplete proton track information, for example, only entry and exit location but not direction, is available.

The expressions published in the previous articles required evaluation of complicated ratios of polynomials. Fur-

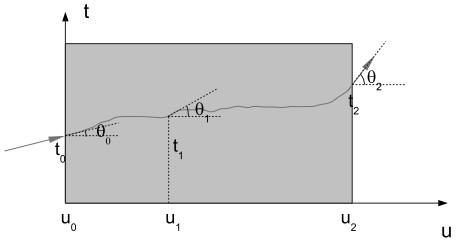

FIG. 1. Scattering geometry in the *u-t* plane.

ther, the expressions were derived for parallel beams and needed to be modified to adapt to incident proton beams with divergent beam direction such as a fan or cone beam. The more compact, matrix-based most likely path formalism presented in this paper uses a scattering model similar to that of Williams but employs Bayesian statistics to determine the lateral displacement and direction of maximum likelihood at any intermediate depth within a uniform absorbing material. Using GEANT4 simulations in a homogeneous water phantom, we demonstrate the performance of the formalism by comparing estimated and simulated proton paths. Further, we demonstrate that the accuracy of the path estimation based on a Gaussian scattering model can be improved by using appropriate angular and energy cuts on the proton histories.

II. MAXIMUM LIKELIHOOD PROTON PATH FORMALISM

The passage of a proton through an object can be described in a semiclassical manner assuming continuous energy loss and scattering, although some of the underlying formulas require quantum mechanics for their derivation.[13] Consider a lab reference system defined by the external detectors of a pCT scanner. The *u*-axis defines the general direction of the proton beam orthogonal to the detector planes and the *t* and *v* axes are parallel to the detector planes. At any given depth u_1 measured along the *u*-axis, the proton can be characterized by its lateral (t_1) and vertical (v_1) coordinates and a lateral and vertical direction characterized by angles θ_1 and φ_1 relative to the *u*-axis. Since scattering in the lateral and vertical direction can be considered as two independent statistical processes, one can confine the derivation of the MLP to one plane, e.g., the *u-t* plane (Fig. 1). In that case, the location and direction of a proton at any depth u_1 is given by the 2D parameter vector,

$$y_1 = \begin{pmatrix} t_1 \\ \theta_1 \end{pmatrix}. \tag{1}$$

Finding the MLP is essentially a maximum likelihood problem, which can be solved within the Bayesian framework. The MLP solution estimates the most likely parameters of a model describing the path (location and direction) of a proton through an object given what is known about the proton from exterior measurements. This can be further developed by including what is known about the object to be reconstructed starting from the prior assumption of an object of water density uniformly filling the reconstruction space and updating the knowledge about the object during iterative steps of the reconstruction. The latter, however, will not be the subject of the current article, as we will maintain the initial assumption of a homogeneous object of water density.

In Bayesian terminology, we have a prior likelihood of finding the proton with a parameter vector y_1 at depth u_1 given some knowledge of the proton before it enters the reconstruction volume, $L(y_1|\text{entry data})$, a likelihood of finding the proton with available exit information given y_1 at depth u_1, $L(\text{exit data}|y_1)$, and a posterior likelihood that the proton had parameters y_1 at depth u_1 given the observed exit information, $L(y_1|\text{exit data})$. According to Bayes' theorem,[14] the prior and posterior likelihood are then related as in Eq. (2),

$$L(y_1|\text{exit data}) = L(\text{exit data}|y_1)L(y_1|\text{entry data}). \tag{2}$$

The most likely location and direction (in short, the MLP) can then be derived by finding the vector y_1 that maximizes the posterior likelihood, thus,

$$L(y_1 = y_{\text{MLP}}|\text{exit data}) = \max, \tag{3}$$

or

$$\nabla L(y_1|\text{exit data}) = \begin{pmatrix} \partial t_1 \\ \partial \theta_1 \end{pmatrix} L(y_1|\text{exit data})|_{y_1=y_{\text{MLP}}} = \begin{pmatrix} 0 \\ 0 \end{pmatrix}. \tag{4}$$

Scattering of a proton in a medium is well described by Moliere's theory;[15] however, for the purpose of the MLP derivation, it is sufficient to use the Gaussian approximation of the generalized Fermi-Eyges theory of MCS,[11] which is an extension of Fermi's original MCS theory.[13] This may be justified by the fact that large-angle scattering events arising both from elastic and nonelastic nuclear interactions, which lead to a non-Gaussian tail of the probability density functions, can be excluded by appropriate data cuts. This process eliminates events with a large relative exit angle, displacements, and/or energy losses. The validity of this assumption was investigated as part of the ensuing simulation work (see Sec. IV).

First, we start with the general form of the likelihood functions involved in proton MCS, assuming that a proton enters the reconstruction volume at u_0 with zero lateral displacement ($t_0=0$) and parallel to the *u*-axis ($\theta_0=0$). In the generalized Fermi-Eyges theory of MCS,[11] the prior likelihood density function of the parameter vector y_1 given the entry information can be described by a bivariate Gaussian, which can be written in compact matrix notation as

$$L\left(y_1|y_0 = \begin{pmatrix} 0 \\ 0 \end{pmatrix}\right) = \exp\left(-\frac{1}{2} y_1^T \Sigma_1^{-1} y_1\right). \tag{5}$$

Here, Σ_1^{-1} is the inverse of the symmetric positive definite scattering matrix whose elements correspond to the variances and covariances of t_1 and θ_1 acquired between u_0 and u_1,

$$\Sigma_1 = \begin{pmatrix} \sigma_{t_1}^2 & \sigma_{t_1\theta_1}^2 \\ \sigma_{t_1\theta_1}^2 & \sigma_{\theta_1}^2 \end{pmatrix}. \tag{6}$$

The elements of the scattering matrix can be calculated from Eqs. (7)–(9) (presented below) and depend on the depth of the proton, taking energy loss into account. These equations, without the logarithmic term, were introduced by Eyges,[11] who solved Fermi's original MCS theory[13] for particles undergoing a significant energy loss. Later, Highland[16] went on to add a logarithmic thickness-dependent correction factor, although their model neglected energy loss and therefore did not contain integrals. The constants used in Eqs. (7)–(9) are based on the refinement of Highland's model by Lynch and Dahl.[17] We followed the suggestion of Gottschalk *et al.*[18] (see their Eq. 29) to extract the logarithmic correction factor out of the integrand. This model was recently shown by Safai *et al.*[19] to accurately describe the lateral profile of collimated and noncollimated proton beams in water when compared to measurements.

In Eqs. (7)–(9), the terms $\beta^2(u)$, $p^2(u)$ are the squared velocity relative to the speed of light c and the momentum of the proton at depth u, respectively, and the empirical constants $E_0=13.6$ MeV$/c$ and 0.038 were introduced by Lynch and Dahl. The quantity X_0 is the radiation length, which is a constant for a given material. Here, we will assume that the scattering object consists of water, for which $X_0=36.1$ cm.

$$\sigma_{t_1}^2(u_0,\ u_1) = E_0^2\left(1+0.038\ln\frac{u_1-u_0}{X_0}\right)^2 \times\int_{u_0}^{u_1}\frac{(u_1-u)^2}{\beta^2(u)p^2(u)}\frac{du}{X_0}, \tag{7}$$

$$\sigma_{\theta_1}^2(u_0,\ u_1) = E_0^2\left(1+0.038\ln\frac{u_1-u_0}{X_0}\right)^2 \times\int_{u_0}^{u_1}\frac{1}{\beta^2(u)p^2(u)}\frac{du}{X_0}, \tag{8}$$

$$\sigma_{t_1\theta_1}^2(u_0,\ u_1) = E_0^2\left(1+0.038\ln\frac{u_1-u_0}{X_0}\right)^2 \times\int_{u_0}^{u_1}\frac{u_1-u}{\beta^2(u)p^2(u)}\frac{du}{X_0}, \tag{9}$$

Let us consider the ideal case that both complete entry information, i.e., lateral coordinate t_0 and angle θ_0 at entry depth u_0, and complete exit information, i.e., lateral coordinate t_2 and angle θ_2 at the exit depth u_2 have been measured. To simplify the MLP derivation, we will make certain small-angle approximations. In particular, by assuming that the entry angle θ_0 is relatively small, i.e., a few degrees, which is realistic for typical pCT entry geometries, we may make use of the small angle approximations; $\sin\theta_0\approx\theta_0$ and $\cos\theta_0\approx 1$.

In order to use the standard form of the Gaussian likelihood given by Eq. (5), we change the local coordinate system of the incoming proton according to the location and orientation of the proton path at the entry depth u_0. In doing so we arrive at an expression for the rotated 2D parameter vector y_1' [Eq. (10)],

$$y_1' = y_1 - R_0 y_0, \tag{10}$$

where

$$R_0 = \begin{pmatrix} 1 & u_1-u_0 \\ 0 & 1 \end{pmatrix}. \tag{11}$$

With this notation, we can define the prior likelihood of y_1 given y_0 as

$$L(y_1|y_0) = \exp\left(-\frac{1}{2}(y_1^T - y_0^T R_0^T)\Sigma_1^{-1}(y_1 - R_0 y_0)\right). \tag{12}$$

Note that an analogous expression, although not in compact matrix form, was derived by Jette *et al.*[20] and applied to electrons undergoing MCS.

It is straightforward to apply the same principle to obtain the likelihood of the exit parameter vector y_2 at depth u_2 given y_1 at depth u_1. Now, justified by the small-angle approximation of MCS, which limits the angle θ_1 to a few degrees, we can define the prior likelihood of y_2 given y_1 as

$$L(y_2|y_1) = \exp\left(-\frac{1}{2}(y_2^T - y_1^T R_1^T)\Sigma_2^{-1}(y_2 - R_1 y_1)\right), \tag{13}$$

where

$$R_1 = \begin{pmatrix} 1 & u_2-u_1 \\ 0 & 1 \end{pmatrix}, \tag{14}$$

and Σ_2^{-1} is the inverse of the positive definite scattering matrix whose elements correspond to the variances and covariances of t_2 and θ_2 acquired between u_1 and u_2. In this case, the scattering elements may be calculated from Eqs. (16)–(18),

$$\Sigma_2 = \begin{pmatrix} \sigma_{t_2}^2 & \sigma_{t_2\theta_2}^2 \\ \sigma_{t_2\theta_2}^2 & \sigma_{\theta_2}^2 \end{pmatrix}, \tag{15}$$

$$\sigma_{t_2}^2(u_1,u_2) = E_0^2\left(1+0.038\ln\frac{u_2-u_1}{X_0}\right)^2\int_{u_1}^{u_2}\frac{(u_2-u)^2}{\beta^2(u)p^2(u)}\frac{du}{X_0}, \tag{16}$$

$$\sigma_{\theta_2}^2(u_1,u_2) = E_0^2\left(1+0.038\ln\frac{u_2-u_1}{X_0}\right)^2\int_{u_1}^{u_2}\frac{1}{\beta^2(u)p^2(u)}\frac{du}{X_0}, \tag{17}$$

$$\sigma_{t_2\theta_2}^2(u_1,u_2) = E_0^2\left(1+0.038\ln\frac{u_2-u_1}{X_0}\right)^2 \times\int_{u_1}^{u_2}\frac{u_2-u}{\beta^2(u)p^2(u)}\frac{du}{X_0}. \tag{18}$$

We can now define the posterior likelihood of y_1 by combining Eqs. (12) and (13) according to Eq. (2),

$$L(y_1|y_2) = \exp\left(-\frac{1}{2}((y_1^T - y_0^T R_0^T)\Sigma_1^{-1}(y_1 - R_0 y_0) + (y_2^T - y_1^T R_1^T)\Sigma_2^{-1}(y_2 - R_1 y_1))\right) \tag{19}$$

$$\equiv \exp(-\chi^2). \tag{20}$$

To derive the MLP, we find the y_1 that minimizes χ^2. First we write

$$\chi^2 = \frac{1}{2}[(y_1^T - y_0^T R_0^T)\Sigma_1^{-1}(y_1 - R_0 y_0) + (y_2^T - y_1^T R_1^T)\Sigma_2^{-1}(y_2 - R_1 y_1)] \tag{21}$$

$$= \frac{1}{2}[y_1^T\Sigma_1^{-1}y_1 - 2y_0^T R_0^T\Sigma_1^{-1}y_1 + y_0^T R_0^T\Sigma_1^{-1}R_0 y_0 + y_2^T\Sigma_2^{-1}y_2 - 2y_1^T R_1^T\Sigma_2^{-1}y_2 + y_1^T R_1^T\Sigma_2^{-1}R_1 y_1]. \tag{22}$$

Carrying out the differentiation of χ^2 with respect to t_1 and θ_1 results in

$$\nabla\chi^2 = (\Sigma_1^{-1} + R_1^T\Sigma_2^{-1}R_1)y_1 - \Sigma_1^{-1}R_0 y_0 - R_1^T\Sigma_2^{-1}y_2. \tag{23}$$

Setting this to zero and solving for y_1, we obtain the following compact maximum likelihood proton path formula:

$$y_{\mathrm{MLP}} = (\Sigma_1^{-1} + R_1^T\Sigma_2^{-1}R_1)^{-1}(\Sigma_1^{-1}R_0 y_0 + R_1^T\Sigma_2^{-1}y_2). \tag{24}$$

A major advantage of the use of the Gaussian approximation of MCS is that the distribution of possible trajectories at a given depth may also be calculated. The inclusion of this error envelope may be an important tool for image reconstruction in pCT. Possible uses that have been suggested include an algorithm that integrates the trajectory likelihood over the volume of each voxel near the proton trajectory or weighting the contribution of a proton trajectory to a voxel solution by some function of the distance in relative units of standard deviations the center of the voxel lies from the trajectory.[12]

The combined t_1 and θ_1 2D Gaussian trajectory distribution can be described by the error matrix ε_{ij}, calculated from the inverse of the curvature matrix α_{ij},

$$\alpha_{ij} \equiv \frac{1}{2}\frac{\partial^2\chi^2}{\partial t_1 \partial\theta_1}, \tag{25}$$

where

$$\frac{\partial^2\chi^2}{\partial t_1\partial\theta_1} = \Sigma_1^{-1} + R_1^T\Sigma_2^{-1}R_1. \tag{26}$$

The error matrix is then found from the inverse of $\alpha_{t1\theta1}$,

$$\varepsilon_{t_1\theta_1}(u_1) = 2(\Sigma_1^{-1} + R_1^T\Sigma_2^{-1}R_1)^{-1}. \tag{27}$$

The element in the first row and first column of $\varepsilon_{t_1\theta_1}(u_1)$ will return the variance in the lateral displacement at a depth u_1.

TABLE I. Results of the polynomial fit to the average value of $1/\beta^2(u)p^2(u)$. The units are c^2/MeV^2 divided by appropriate powers of cm.

Coefficients	Values
a_0	7.457×10^{-6}
a_1	4.548×10^{-7}
a_2	-5.777×10^{-8}
a_3	1.301×10^{-8}
a_4	-9.228×10^{-10}
a_5	2.687×10^{-11}

III. GEANT4 SIMULATIONS

In order to calculate the elements of the scattering matrices [Eqs. (7)–(9) and (16)–(18)], one requires knowledge of how the proton loses energy with depth in a material. In particular, we require

$$\frac{1}{\beta^2(u)p^2(u)} = \frac{(E(u)+E_p)^2c^2}{(E(u)+2E_p)^2E^2(u)}. \tag{28}$$

In Eq. (28), β is the velocity of the proton relative to the speed of light, p is the momentum, $E(u)$ is the depth-dependent kinetic energy, and $E_p = 938.272\ \mathrm{MeV}/c^2$ is the proton rest energy. For this section, a simple GEANT4 (Ref. 21) simulation was carried out with a 200 MeV monoenergetic proton pencil beam incident on a 20 cm thick water absorber. The mean value of $1/\beta^2p^2$ of the protons was recorded in 5 mm intervals through the absorber. A fifth-degree polynomial was fit to these data to provide a $1/\beta^2(u)p^2(u)$ function as suggested by Williams.[12] Approximating $1/\beta^2(u)p^2(u)$ with a polynomial allows for an explicit evaluation of the integral form of the scattering elements, avoiding the use of numerical integration methods,

$$\frac{1}{\beta^2(u)p^2(u)} = a_0 + a_1u + a_2u^2 + a_3u^3 + a_4u^4 + a_5u^5. \tag{29}$$

The coefficients of the fifth-degree polynomial fit to $1/\beta^2(u)p^2(u)$ derived from the GEANT4 data are listed in Table I.

In order to study the performance of Eq. (24) as an MLP formula, the Monte Carlo proton tracks of a GEANT4 simulation were compared to the output of the derived MLP. Simulating clinical pCT conditions, a monoenergetic, uniformly distributed proton fan beam of 200 MeV was incident on a 20 cm water cube. As mentioned above, since scattering in the lateral and vertical direction can be considered as two independent statistical processes, beam divergence was fixed to the *t-u* plane (Fig. 2). Sensitive volumes were installed at the entry and exit faces of the cube and at 5 mm intervals throughout the cube to record the projection of the displacement and angle of the 3D Monte Carlo tracks onto the *t-u* plane for each proton history. Proton energy was also recorded at the exit face.

The simulations were carried out based on the GEANT4 multiple scattering model, low energy hadronic ionizations, low energy hadronic elastic collisions, and ICRU-based low energy inelastic collision models. The first 3000 protons to

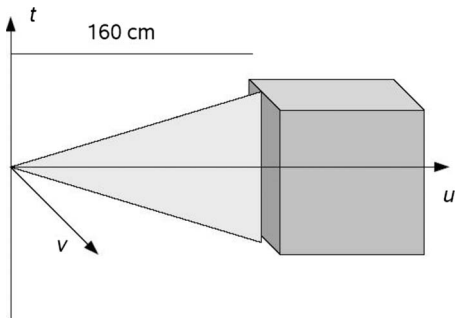

FIG. 2. Geometry of the GEANT4 simulation. The incident beam has no width in the u-v plane and a uniform fan distribution in the u-t plane.

completely traverse the cube were recorded for analysis. As well as recording proton position, direction, and energy, the GEANT4 toolkit also allowed for an identification of protons that underwent a nuclear collision (elastic or inelastic) at any stage through the object.

Following the simulation, the mean and standard deviation (σ) of the relative exit angle (difference between proton exit and entry angle) and exit energy of the recorded histories were calculated. This allowed for the implementation of 3σ data cuts where protons having a relative exit angle or exit energy lying more than 3σ from the respective means were eliminated. The effect of these cuts on MLP performance was investigated.

IV. RESULTS

Figure 3 demonstrates three examples of proton Monte Carlo tracks in water obtained from GEANT4, as well as the MLP [Eq. (24)] with associated error envelopes [Eq. (27)]. Figures 3(a) and 3(b) illustrate how the MLP smoothes out the many individual small-angle scattering events. Figure 3(c) gives an example of a history that was identified to have undergone an elastic nuclear collision. The effect of such an event on path accuracy is evident. Note that the examples in Fig. 3 were generated with protons inclined to the u-axis.

A plot of the root-mean-square (rms) error in lateral displacement as a function of depth in water for the 3000 proton histories analyzed can be seen in Fig. 4. The three plots illustrate the effect of the analyzed nuclear collision events (>99% of which are elastic collisions) on the overall accuracy of the derived formula. Recall that Eq. (24) was formulated assuming a Gaussian distribution of multiple scattering, and as such will only be accurate for events that undergo small-angle MCS. So, in order to minimize the effect of elastic nuclear collision and large-angle MCS events in pCT image reconstruction, 3σ cuts on the relative exit angle (difference between proton exit and entry angle) should be performed. Further, in a clinical pCT system, secondary protons may be generated within the imaged object through inelastic nuclear collisions. In order to eliminate these and the primary protons taking part in the reaction, 3σ cuts on the exit energy should also be performed to maximize density resolution.[8] The best practically achievable plot, obtained by performing these cuts, was found to display a maximum rms

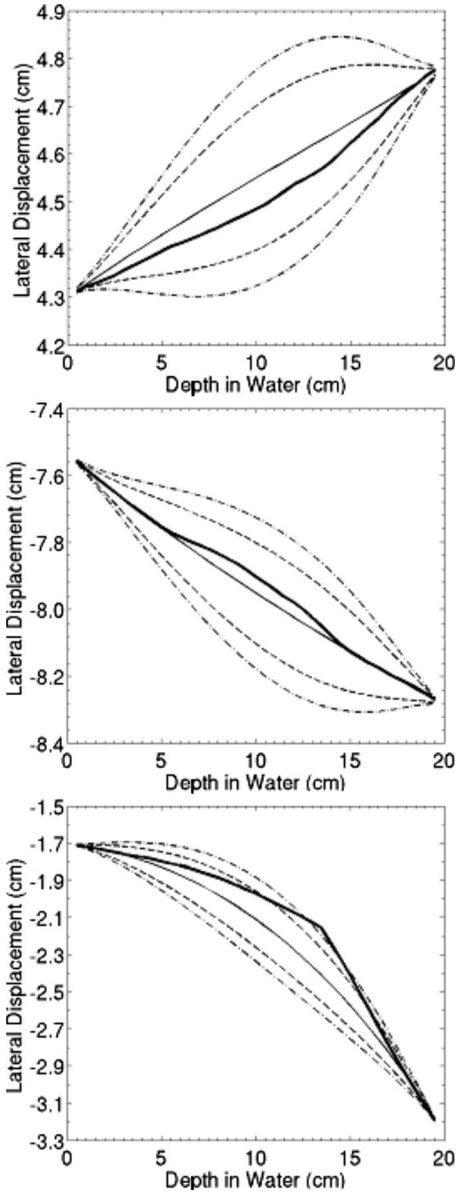

FIG. 3. Examples of off-axis oblique Monte Carlo proton tracks (bold) and MLP output (solid line) with associated 2 (dash-dash-dash) and 3σ (dash-dot-dash) error envelopes. The top two Monte Carlo tracks underwent MCS only and lie completely within the error envelopes. The bottom example shows a proton that underwent an elastic nuclear collision and falls outside both error envelopes.

error of approximately 0.55 mm at the center of the water object.

The effect of the aforementioned cuts on MLP performance is also demonstrated in Table II. Because a Gaussian approximation of multiple scattering was utilized, it would be expected that ~1% and 5% of events would fall outside the $3\sigma_{\mathrm{MLP}}$ and $2\sigma_{\mathrm{MLP}}$ error envelopes, respectively, if only small-angle scattering events were recorded. However, because nuclear collision events were also included in the simulation and a non-Gaussian model of MCS is employed in GEANT4, values of 8.47% and 13.47% were found for these quantities respectively if no cuts were performed. If 3σ cuts on the relative exit angle and exit energy are used, elimi-

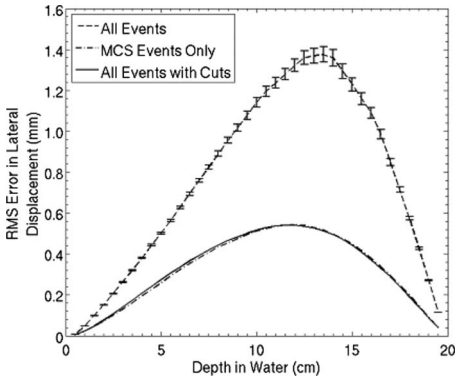

FIG. 4. Root-mean-square (rms) error in lateral displacement in the *t-u* plane between the path approximation formula and associated Monte Carlo track as a function of depth in water for 3000 GEANT4 proton histories. Error bars were not included for the rms multiple scattering and cuts plots, as the errors were negligible.

nating the majority of the large-angle scattering events, these values are reduced to 1.87% and 6.38%, much closer to the expected ~1% and 5%. Table II also demonstrates that the majority of events lying outside the error envelopes are eliminated by the relative exit angle cut and not greatly improved by the exit energy cut. As already mentioned, the energy cuts are necessary, however, for optimal density resolution in pCT.

V. DISCUSSION

A new formalism of deriving the MLP of a charged particle in a uniform material within the Bayesian maximum likelihood framework has been proposed. The MLP formula derived in this article was applied to scenarios where the position and direction of each proton at the entry and exit planes are known, but a case with more restricted information is presented in the Appendix. The simulation toolkit GEANT4 was used to compare Monte Carlo proton tracks to the output of the derived MLP expression. It was found that the new formalism could predict the Monte Carlo paths based on the entry and exit information to within 0.6 mm on average when applying 3σ cuts on the relative exit angle of the protons. Such cuts were found to eliminate the majority of events that did not conform to the Gaussian approximation of MCS employed in the derivation (i.e., nuclear collisions or large-angle MCS) and thus improve the path approximation accuracy. Eliminating these events is advantageous for pCT image reconstruction purposes where the greatest spatial resolution will be achieved when proton path approximation is at its most accurate. Additional 3σ cuts on exit energy did only slightly improve the performance of the formalism; however, these cuts are valuable to properly reconstruct the relative electron density integrated along the proton path.[8]

From the plots in Fig. 4 it can be seen that the largest error in path approximation, on average, occurs downstream from the center of the object as previously described by Schneider and Pedroni.[10] This suggests that pCT images will exhibit less spatial resolution in the paracentral region of the image. Application of the standard deviation of the proton displacement around the MLP, which can be derived from the error matrix [Eq. (27)], may prove advantageous in dealing with this. In present reconstruction work,[9] the proton path is assumed to be deterministic by giving it a weight of 1 in voxels that are intersected by the MLP and zero elsewhere. By using a probability rather than a binomial value (0, 1), an improvement in spatial resolution at depth in pCT images may be achieved.

The Bayesian formulation with compact matrix formulation presented in this work is also applicable to incomplete track information. In the Appendix, we present an example where the proton direction at the exit plane is unknown and the proton direction in the entry plane is approximately inferred from knowledge of the beam divergence. Using the likelihood formulation of the MLP, it is straightforward to derive the case-specific MLP. This approach will be adopted for a small-scale cone beam prototype pCT system currently being developed at Loma Linda University Medical Center (LLUMC), California. The prototype system features only two 2D sensitive tracking modules, limiting the information available about proton trajectories.

Throughout this work it has been assumed that that the reconstruction space between the detection planes is filled by the object of water density. In clinical pCT situations, however, there will be an air gap up to a few tens of centimeters

TABLE II. Summary of the effect of applying various cuts on the MLP performance. Note that if at any stage through the water cube a track was found to have a greater error than the width of a σ_{MLP} envelope, it was identified as falling outside the error envelope.

		Type of cut	% of tracks lying outside σ_{MLP} envelope after applying cut
Envelope width	$2\sigma_{MLP}$	None	13.47
		3σ exit energy	10.79
		3σ relative exit angle	6.52
		3σ exit energy and 3σ relative exit angle	6.38
	$3\sigma_{MLP}$	None	8.47
		3σ exit energy	5.88
		3σ relative exit angle	1.89
		3σ exit energy and 3σ relative exit angle	1.87

between patient and position sensitive detectors. An assumption of homogeneous material filling of the reconstruction space thereby renders the MLP inaccurate to a certain degree. It is possible, in principle, to deal with this issue when using iterative reconstruction techniques. With such algorithms, the knowledge of the reconstruction space is updated after each iteration cycle. In our experience, the object boundary is clearly visible after the first cycle. Considering this, we suggest that, for the purposes of the MLP calculations, the entire reconstruction volume is assumed to be homogeneous water only in the first cycle. A simple border detection algorithm can then be used to determine scattering object boundaries. Using this information, the MLP calculation can be subdivided into the following cycles. The first and last sections of the proton path (outside the object) would use the radiation length of air in Eqs. (7)–(9) and (16)–(18) with negligible energy loss, while the intermediate section (inside the object) would make use of the values outlined in the simulation work presented here. Furthermore, simulations presented here have only considered scattering in homogeneous water, while in real pCT cases the object to be imaged will be of an initially unknown inhomogeneous composition. This can be dealt with in a manner similar to the air gap issue described above. Once again, iteratively updated information about the density distribution of the object after complete iterations in the reconstruction process can be used to iteratively update the MLPs in successive iterations. This implies a large computational effort that needs to be addressed both on the soft- and hardware level.

VI. CONCLUSION

A new formalism for calculating the proton path of maximum likelihood for application in pCT image reconstruction has been proposed. The matrix-based formalism is mathematically equivalent to the previously presented MLP formalisms by Schneider and Pedroni[10] and Williams[12] but is more compact, independent of incident beam geometry, and can be adapted to different pCT detector configurations. In a homogeneous 20 cm water cube, the method was found to be able to predict the Monte Carlo tracks of 200 MeV protons to within 0.6 mm on average when employing 3σ cuts on the relative exit angle and exit energy. These cuts were found to eliminate the majority of events not conforming to the Gaussian model of MCS used in the MLP derivation.

ACKNOWLEDGMENT

The authors would like to thank William Preston, Ed.D. for editorial assistance.

APPENDIX: EXAMPLE FOR AN MLP BASED ON ENTRY AND EXIT LOCATION AND CONE BEAM GEOMETRY

Consider a pCT system where only position is known at the entry and exit planes of the reconstruction volume. Further, because a cone beam is employed, entry direction can be inferred from the entry location via the relationship between cone beam focus and entry location. For a cone beam of relatively small divergence, we have $\theta_0 \cong t_0/d$, where d is the distance of the entry plane from the beam focus. In this case, the prior likelihood of measuring a proton with parameter vector y_1 at depth u_1 given the entry parameter vector $y_0=(t_0,t_0/d)^T$ at the entry plane is defined as for the case of complete entry information [Eq. (12)].

The likelihood of observing the exit location t_2 given the parameter vector y_1 at intermediate depth u_1 is derived by marginalization of the likelihood $L(y_2|y_1)$ in Eq. (13). Integrating over all possible angles θ_2, we have

$$L(t_2|y_1)=\int_{-\infty}^{\infty}L(y_2|y_1)d\theta_2 = \exp\left(-\frac{1}{2}\frac{(t_2-t_1-\theta_1(u_2-u_1))^2}{\sigma_{t_2}^2}\right), \tag{A1}$$

where $\sigma_{t_2}^2$ is given by Eq. (16). Compact matrix notation can be reintroduced by writing

$$L(t_2|y_1)=\exp\left[-\frac{1}{2}\frac{(y_2^T-y_1^TR_1^T)\nu\nu^T(y_2-R_1y_1)}{\sigma_{t_2}^2}\right], \tag{A2}$$

where the auxiliary vector $\nu=(1,0)^T$. Combining this with the prior likelihood, one obtains the posterior likelihood $L(y_1|t_2)$, where the χ^2 exponent is given by

$$\chi^2=\frac{1}{2}\left[(y_1^T-y_0^TR_0^T)\Sigma_1^{-1}(y_1-R_0y_0) + \frac{(y_2^T-y_1^TR_1^T)\nu\nu^T(y_2-R_1y_1)}{\sigma_{t_2}^2}\right]. \tag{A3}$$

Differentiating χ^2 with respect to y_1 and collecting terms in y_1, we obtain

$$\nabla\chi^2=\left(\Sigma_1^{-1}+\frac{R_1^T\nu\nu^TR_1}{\sigma_{t_2}^2}\right)y_1-\Sigma_1^{-1}R_0y_0-\frac{R_1^T\nu\nu^Ty_2}{\sigma_{t_2}^2}. \tag{A4}$$

Introducing the notation

$$y_2'\equiv R_1^T\nu\nu^Ty_2=t_2\begin{pmatrix}1\\u_2-u_1\end{pmatrix} \tag{A5}$$

and

$$R_1'\equiv R_1^T\nu\nu^TR_1=\begin{pmatrix}1 & u_2-u_1\\ u_2-u_1 & (u_2-u_1)^2\end{pmatrix}, \tag{A6}$$

we have

$$\nabla\chi^2=\left(\Sigma_1^{-1}+\frac{R_1'}{\sigma_{t_2}^2}\right)y_1-\Sigma_1^{-1}y_0R_0-\frac{y_2'}{\sigma_{t_2}^2}. \tag{A7}$$

Setting $\nabla\chi^2=0$ and solving for y_1, the following expression for the MLP with known entry and exit location and cone beam geometry is obtained:

$$y_{\mathrm{MLP}}=\left(\Sigma_1^{-1}+\frac{R_1'}{\sigma_{t_2}^2}\right)^{-1}\left(\Sigma_1^{-1}R_0y_0+\frac{y_2'}{\sigma_{t_2}^2}\right). \tag{A8}$$

[a]Author to whom correspondence should be addressed. Electronic mail:

rschulte@dominion.llumc.edu; Telephone: 909-558-4243.

[1]A. M. Cormack, "Representation of a function by its line integrals, with some radiological applications," J. Appl. Phys. **34**, 2722 (1963).
[2]A. M. Koehler and V. W. Steward, "Proton beam radiography in tumor detection," Science **179**, 913–914 (1973).
[3]A. M. Koehler and V. W. Steward, "Proton radiographic detection of strokes," Nature (London) **245**, 38–40 (1973).
[4]D. R. Moffett, E. P. Colton, G. A. Concaildi, E. W. Hoffman, R. D. Klem, M. J. Knott, S. L. Kramer, R. L. Martin, E. F. Parker, A. R. Passi, P. F. Schultz, R. L. Stockley, R. E. Timm, L. S. Skaggs, and V. W. Steward, "Initial test of a proton radiographic system," IEEE Trans. Nucl. Sci. **3**, 1749–1751 (1975).
[5]K. M. Hanson, J. N. Bradbury, T. M. Cannon, R. L. Hutson, D. B. Laubacher, R. J. Macek, M. A. Paciotti, and C. A. Taylor, "Computed tomography using proton energy loss," Phys. Med. Biol. **26**, 965–983 (1981).
[6]K. M. Hanson, J. N. Bradbury, R. A. Koeppe, R. J. Macek, D. R. Machen, R. Morgado, M. A. Paciotti, S. A. Sandford, and V. W. Steward, "Proton computed tomography of human specimens," Phys. Med. Biol. **27**, 25–36 (1982).
[7]P. Zygmanski, K. P. Gall, M. S. Z. Rabin, and S. J. Rosenthal, "The measurement of proton stopping power using proton-cone-beam computed tomography," Phys. Med. Biol. **45**, 511–528 (2000).
[8]R. W. Schulte, V. Bashkirov, M. C. Klock, T. Li, A. J. Wroe, I. Evseev, D. C. Williams, and T. Satogata, "Density resolution of proton computed tomography," Med. Phys. **32**, 1035–1046 (2005).
[9]T. Li, L. Zhengrong, J. V. Singanallur, T. J. Satogata, D. C. Williams, and R. W. Schulte, "Reconstruction for proton computed tomography by tracing proton trajectories: A Monte Carlo study," Med. Phys. **33**, 699–706 (2006).
[10]U. Schneider and E. Pedroni, "Multiple Coulomb scattering and spatial resolution in proton radiography," Med. Phys. **21**, 1657–1663 (1994).
[11]L. Eyges, "Multiple scattering with energy loss," Phys. Rev. **74**, 1534–1535 (1948).
[12]D. C. Williams, "The most likely path of an energetic charged particle through a uniform medium," Phys. Med. Biol. **49**, 2899–2911 (2004).
[13]B. Rossi and K. Greisen, "Cosmic-ray theory," Rev. Mod. Phys. **13**, 240–268 (1941).
[14]S. M. Stigler, "Thomas Bayes' Bayesian inference," J. R. Stat. Soc. Ser. A (Gen.) **145**, 250–258 (1982).
[15]H. A. Bethe, "Molière's theory of multiple scattering," Phys. Rev. **89**, 1256 (1953).
[16]V. L. Highland, "Some practical remarks on the multiple scattering," Nucl. Instrum. Methods **129**, 497–499 (1975). Also see: V. L. Highland, Nucl. Instrum. Methods **161**, 171 (1979) (erratum).
[17]G. R. Lynch and O. I. Dahl, "Approximations to multiple Coulomb scattering," Nucl. Instrum. Methods Phys. Res. B **58**, 6–10 (1991).
[18]B. Gottschalk, A. M. Koehler, R. J. Schneider, J. M. Sisterson, and M. S. Wagner, "Multiple Coulomb scattering of 160 MeV protons," Nucl. Instrum. Methods Phys. Res. B **74**, 467–490 (1993).
[19]S. Safai, T. Bortfeld, and S. Engelsman, "Comparison between the lateral penumbra of a collimated double-scattered beam and uncollimated scanning beam in proton radiotherapy," Phys. Med. Biol. **53**, 1729–1750 (2008).
[20]D. Jette, L. H. Lanzl, and M. Rozenfeld, "The application of multiple scattering theory to therapeutic electron dosimetry," Med. Phys. **10**, 141–146 (1983).
[21]S. Agostinelli *et al.*, "GEANT4—A simulation toolkit," Nucl. Instrum. Methods Phys. Res. A **506**, 250–303 (2003).